A Letters Journal Exploring the Frontiers of Physics

June 2008

EPL, **82** (2008) 67002
doi: 10.1209/0295-5075/82/67002

www.epljournal.org

Doping-dependent phase diagram of LaOMAs (M = V–Cu) and electron-type superconductivity near ferromagnetic instability

G. Xu[1], W. Ming[1], Y. Yao[1], X. Dai[1], S.-C. Zhang[2] and Z. Fang[1(a)]

[1] *Beijing National Laboratory for Condensed Matter Physics, Institute of Physics, Chinese Academy of Sciences Beijing 100190, China*
[2] *Department of Physics, Stanford University - Stanford, CA 94305-4045, USA*

received 21 April 2008; accepted 29 April 2008
published online 3 June 2008

PACS 74.70.-b – Superconducting materials
PACS 74.25.Jb – Electronic structure
PACS 74.25.Ha – Magnetic properties

Abstract – By first-principles calculations, we present a doping-dependent phase diagram of the LaOMAs (M = V–Cu) family. It is characterized as a antiferromagnetic semiconductor around the LaOMnAs side and as a ferromagnetic metal around LaOCoAs. Both LaOFeAs and LaONiAs, where superconductivity were discovered, are located at the borderline of magnetic phases. An extensive Fermi surface analysis suggests that the observed superconductivity is of electron type in its origin. We discuss possible pairing mechanisms in the context of competing ferromagnetic phases found in this work and the ferromagnetic spin fluctuations.

The studies on new superconductors, particularly non-cuperate layered compounds, are always exciting and offer new perspectives for the possible further raising of the transition temperature T_c. Except for few of the non-transition-metal compounds, such as MgB_2, where superconductivity with T_c up to 39 K was found [1], problems in many cases are as complicated and challenging as we found in cuperates. In the layered ruthenates, the ferromagnetic spin fluctuation is important and a spin-triplet p-wave character was suggested [2] for the superconductivity found in Sr_2RuO_4 with $T_c \sim 1$ K [3]. In a more recent example, $Na_xCoO_2 \cdot (H_2O)_y$ [4], the geometry fluctuations due to triangle lattice are extensively discussed [5]. Here we will show that a rich doping-dependent phase diagram can be realized in the new family of layered compounds LaOMP or LaOMAs (M = V–Cu), where up to $T_c = 26$ K superconductivity was reached very recently in LaOFeAs after F^--doping [6–8].

The quaternary oxypnictides LaOMAs crystallize in a layered tetragonal structure with $P4/nmm$ symmetry [9]. Each transition metal (oxygen) layer is sandwiched by two nearest-neighbor As (La) atomic layers, which form edge-shared tetrahedrons around the M (oxygen) sites. The $(M\text{As})^-$ and $(\text{LaO})^+$ triple-layer subgroups stack alternatively along the c-axis. The positions of La or As sheets are determined by two internal parameters, z_{La} and z_{As}, which define the inter-layer distances of La-O and M-As, respectively. It is important that this series of compounds are chemically stable such that systematical tuning is available without altering the structure and symmetry significantly. For instance, a variety of compounds can be synthesized by the replacement of transition metal elements, where both the electron doping and hole doping can be realized by replacing O^{2-} or La^{3+} ions. Except for the early report for the structure study [9], the detailed studies on the electronic and magnetic properties for this series of compounds are still in their early stage. It was first reported in 2006 that superconductivity can be realized in LaOFeP below 4 K, and T_c was increased to 7 K by F-doping [6]. Later, superconductivity with T_c about 2 K was reported for LaONiP [7], and T_c around 26 K was reached very recently in LaOFeAs again after F-doping [8]. We will present in this letter that both M = Fe and Ni compounds locate at special positions of the global phase diagram for the series of M-substituted compounds. The competing magnetic and superconducting phases found in our global phase diagram provide important clues on the possible pairing mechanism in this class of materials.

The phase diagram is constructed from first-principles calculations based on density functional theory with generalized gradient approximation (GGA) of PBE type [10] for the exchange correlation potential. We use

(a) E-mail: zfang@aphy.iphy.ac.cn

Table 1: The optimized lattice parameters (a and c), the internal coordinates ($z_{\rm La}$ and $z_{\rm As}$), and the calculated specific heat coefficient γ_0 and bare susceptibility χ_0 for the series of compounds LaOMAs in the NM state.

	a (Å)	c (Å)	$z_{\rm La}$	$z_{\rm As}$	$\gamma_0\left(\frac{\rm mJ}{k^2{\rm mol}}\right)$	$\chi_0\left(10^{-5}\frac{\rm emu}{\rm mol}\right)$
V	3.9965	9.3655	0.1367	0.1643	7.47	10.25
Cr	3.9355	9.3467	0.1397	0.1592	9.06	12.43
Mn	4.0355	8.7822	0.1438	0.1427	11.37	15.59
Fe	4.0396	8.6289	0.1461	0.1369	5.52	7.57
Co	4.0621	8.5434	0.1466	0.1369	7.41	10.17
Ni	4.1404	8.3139	0.1466	0.1366	3.81	5.23
Cu	4.1442	8.5681	0.1424	0.1539	3.98	5.46

the plane-wave pseudopotential method, and the ultra-soft pseudopententail scheme [11] is adopted. The convergence of total-energy calculations with respect to the number of K-points and the cut-off energy (of plane-wave expansion) is well checked, and final results are double-checked using the full-potential linearized augmented plane-wave (FLAPW) method (WIN2K package) [12]. The series of LaOMAs compounds with M ranging from V to Cu are all studied with full lattice optimizations using experimental 2-Fe cell, and the non-magnetic (NM), ferromagnetic (FM), and (intra-layer) antiferromagnetic states are treated. The same approach has been also applied to the LaOMP series, qualitatively the same results are obtained, we therefore concentrate our following discussions on the LaOMAs series for consistence.

As shown in table 1, the optimized lattice parameters and internal coordinates for Fe and Ni compounds are in excellent agreement with the available experimental data [6–9], which demonstrates the quality of our present calculations. The optimized parameters are used in our calculations for all the compounds. Moving from V to Cu, the lattice parameters are only slightly modified, despite the dramatical change of the number of 3d electrons (from d^3 of V^{2+} to d^9 of Cu^{2+}), suggesting the less sensitivity of the lattice distortion.

Figure 1 shows the phase diagram computed for the whole range of compounds. The solid lines and the dashed lines represent the stabilization energies of the FM and AF states relative to the NM solution, respectively. Two distinct phase regions can be identified: the dome below Fe gives the AF ground state, while the one around Co is ferromagnetic. The computed magnetic moments (see fig. 1) show that the left-hand-side AF phase region is strongly spin polarized, while the magnetic moment of the ferromagnetic phase around Co is small, suggesting possibly different origins of the two magnetic-phase regions. It is important to note that both LaOFeAs and LaONiAs are located at special positions of the phase diagram: the Fe compound is at the borderline between the AF and FM phase regions; while the Ni compound is at the other border of the FM phase. The overall phase diagram clearly suggests that the magnetic instabilities are crucially important to understand the physical properties

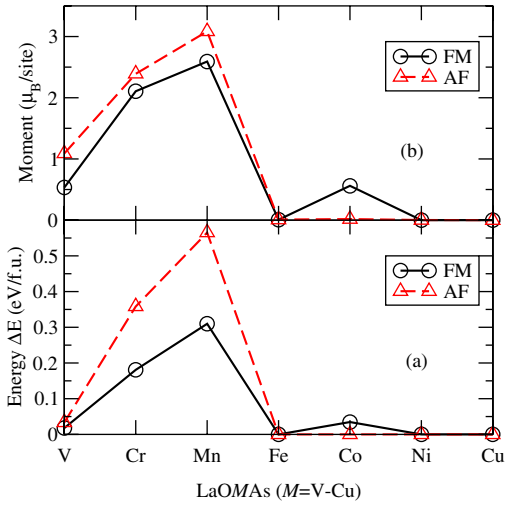

Fig. 1: Phase diagram: (a) the calculated stabilization energies of the FM and AF states with respect to the NM state for various compounds with increasing number of 3d electrons; (b) the corresponding magnetic moments obtained from calculations.

of this new family of compounds. The present calculations are done based on the experimental crystal cell with 2 Fe per cell [8]. However, we notice that a strong nesting effect exists particularly for LaOFeAs. This will lead to the stripe-type spin-density-wave (SDW) ground state with a $\sqrt{2}\times\sqrt{2}$ super-cell structure. The detailed results for this SDW state will be presented in a separate paper combined with experimental results [13].

To understand the electronic structures, we show the total and projected density of states (DOS) of various compounds in fig. 2. Let us start from LaOFeAs (fig. 2(a)). The states between -2 eV and $+2$ eV are mostly from Fe-3d states, just below which are the states of O-p and As-p (from -6 eV to -2 eV). The p-d hybridization between O and Fe is negligible, while that between As and Fe is sizable. This As-M p-d hybridization is enhanced by changing to the Ni compound (see the projected DOS of fig. 2(b)). Since the transition metal sites are coordinated by the As-tetrahedron, the crystal field will normally splits the five d orbitals into low-lying twofolds e_g states and up-lying threefolds t_{2g} states. However, the As-tetrahedron is actually much distorted from its normal shape (squeezed along c by about 20%). This distortion will further split the e_g and t_{2g} manifolds significantly making the final orbital distributions complicated. As a result, what actually happens is opposite to what we expect from a simple tetrahedra crystal field: the low-lying manifold is threefold and the higher-lying manifold is twofold, between which a pseudo-gap of about 0.5 eV exists. For the Fe compound, the nominal number of d electrons is 6, and the low-lying threefold bands are nearly fully occupied with the Fermi level E_f located very close to the deep of the pseudo-gap. If the crystal field is strong enough, which may be achieved by the substitution of As atoms, a simple band insulator will be expected

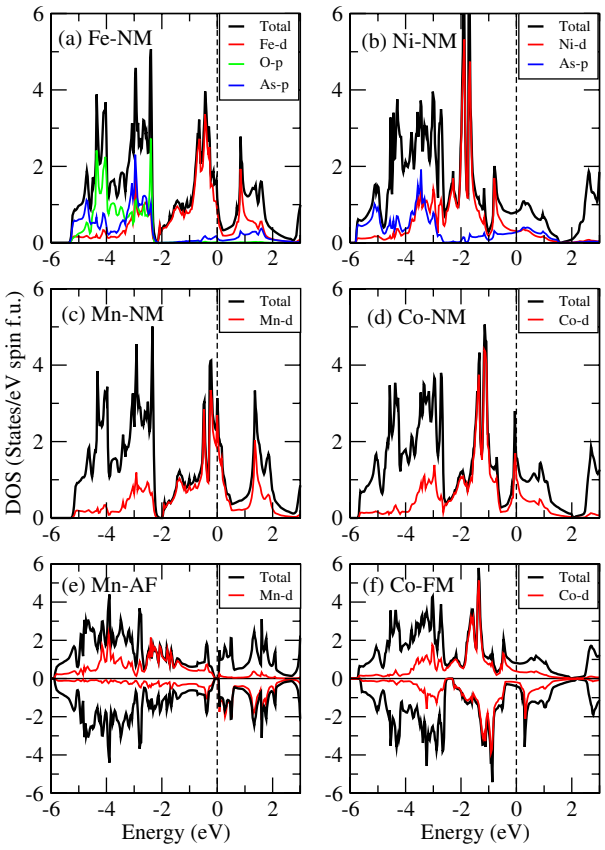

Fig. 2: The calculated electron density of states (DOS) for various compounds in different states (see text for the explanation).

by enlarging the pseudo-gap. From the calculated DOS at E_f, we estimate the bare susceptibility and specific heat coefficient, which are $\chi_0 = 7.6 \times 10^{-5}$ emu/mol and $\gamma_0 = 5.5\,\mathrm{mJ/K^2}$ mol for the Fe compound (see table 1 for other compounds). Taking the experimental susceptibility of about 50×10^{-5} emu/mol at 300 K, a renormalization factor of about 6.6 is suggested, which is close to that shown in Sr_2RuO_4 [14].

Moving to the Mn compound, the half-filled d-shell (about d^5) will gain energy from Hund's coupling, and the spin-polarized states will be favored as results. In reality, the calculated total energies of both FM and AF solutions are much lower than that of the NM solution (about 0.3 eV/f.u. for the former and 0.55 eV for the latter). The reason why the AF solution is more favored is that a gap of about 0.2 eV is opened in the AF solution (see fig. 2(e)). It is mentioned (but without showing data) in the recent experimental paper [6] that LaOMnP is a semiconductor. This is consistent with our prediction, and further we show that the ground state of the Mn compound is AF. The calculated spin moment is about $3.1\,\mu_B$/Mn which is much reduced from the expected $5\,\mu_B$/Mn of a high-spin state. There are two possibilities to explain the reduced moment. One is that Mn is in an intermediate spin state rather than in a high-spin state. If this is the case, certain kinds of orbital ordering would be expected for an AF insulator. However, our calculated occupation numbers of the projected 3d-shell orbitals are quite uniform, suggesting that this possibility is unlikely. The second possibility is due to either p-d or d-d hybridization (particularly for a narrow-gap system). The calculated spin moment is about $4.3\,\mu_B$/Mn for a typical high-spin AF insulator MnO [15], where only the p-d hybridization is important. However, here we point out that the Mn-Mn distance in LaOMnAs is about 2.8 Å, which is much shorter than what was found in MnO (about 3.2 Å), and is actually very close to the distance in elementary Mn (about 2.6–2.7 Å). The direct d-d hybridization will be much enhanced by such short distance, which will again reduce the moment. The effect of direct d-d overlap has been addressed in a previous study for LaOFeP [16]; however we emphasize here that this is generally true for all the compounds of this family as shown by the optimized structure (table 1).

The stabilization of the FM phase region on the right-hand side has a different origin as will be discussed here for LaOCoAs. Co has one more d electron than Fe, therefore the Fermi level is lifted up and located above the pseudo-gap. What is interesting is that a strong Van Hove singularity (VHS) is present just at the Fermi level of LaOCoAS NM DOS as shown in fig. 2(d). The high $N(E_f)$ in the presence of this VHS will push the system to be itinerant FM due to the Stoner instability. This mechanism is further supported by the following factors: 1) the FM region is relatively narrow; 2) the polarized spin moment is small (about $0.5\,\mu_B$/Co); 3) the energy gain is also small (about 35 meV/f.u.). By adding one more electron, for LaONiAs, the Fermi level is shifted away from the VHS, the system is recovered to be NM again as shown in the phase diagram.

Having finished the discussions for the phase diagram and the general picture of the electronic structure, now let us focus on LaOFeAs and LaONiAs, where superconductivity is discovered. Figure 3 gives the calculated band structures and Fermi surfaces (FS) for both compounds (the window for d-bands is shown, and there are totally ten d-bands in our unit cell). First of all, the band dispersions along the z-direction are all very weak suggesting the 2-dimensional nature of those compounds. Considering the in-plane dispersions, the band structure of LaOFeAs can be schematically separated into two parts. The bands below E_f are relatively flat and have little contribution coming from the As-p states, while the bands above E_f are quite dispersive (except for some flat branches around +1 eV which correspond to the VHS discussed above), and have large weight coming from the As-p character (as shown by the projected fat-bands plot). Those dispersive bands form electron-like FS cylinders around the M-A lines of the Brillouin zone, and hole-like FS cylinders are formed around the Γ-Z lines due to the Fermi level crossing of the bands from the lower part. For LaONiAs, all the flat bands are pushed down to below the Fermi level, and only the dispersive bands remain to cross the Fermi level,

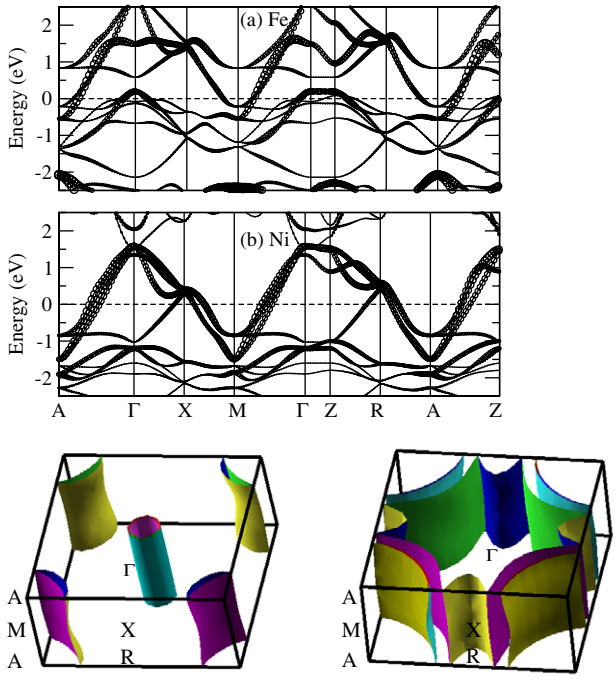

Fig. 3: The calculated band structures of (a) LaOFeAs and (b) LaONiAs. The fat bands are shown with projection to As-p states. The lower panels show the calculated Fermi surfaces of LaOFeAs after 10% F-doping (left) and LaONiAs (right).

which give the large electron FS around the M-A lines, but a hole-type FS around the X-R line instead of the Γ-Z one.

The experimental results show that LaOFeAs is superconducting only after electron-type F-doping [8], and also T_c of LaOFeP (which has very similar band structure [16] as LaOFeAs) is enhanced with F-doping [6]. All those evidences suggest that the electron-like FS formed by the dispersive band should be responsible for the superconductivity. Taking the calculated total DOS of LaOFeAs, the $N(E_f)$ will decrease with up-shifting of the Fermi level, contrary to the experimental trend observed for F-doping. However, if we only take into account the contribution from the electron-like FS, its DOS will increase with increasing Fermi energy. Actually, as shown in fig. 3, the hole-like FS of LaOFeAs after 10% F-doping are much reduced, and electron-like FS are enlarged, compared to the case without doping [16]. The very recent Hall measurements also suggested the electron-type conductivity in LaONiAs after F-doping [17].

Up to now, superconductivity has been discovered in several transition metal systems, including the cuperates, ruthenates and cobaltates. Most of these superconducting materials are hole doped and only a few of them are electron doped. In cuperates, the electron-doped compounds usually have much lower T_c than the hole-doped ones. In sodium cobaltates, only hole-doped compounds are realized. The present systems are also layered compounds, and the p-d hybridization is sizable. Considering the close vicinity to the ferromagnetic instability, the present systems are very similar to Sr_2RuO_4, where strong ferromagnetic fluctuations favor triplet pairing. In such case, the question is whether the pairing state is unitary and time-reversal invariant, analogously to the B-phase of ^{3}He, or non-unitary and time-reversal breaking, analogously to the A-phase of ^{3}He [18]. Our calculations show that LaOFeAs can be basically characterized as low-electron-density carriers doped on top of a band insulator with filled d^6 valence orbitals. In ^{3}He, the B-phase is realized under the low- or ambient-pressure condition, while the A-phase is realized under the high-pressure condition close to solidification. By analogy, we suggest that the low-electron-density system LaOFeAs is in the weak-coupling limit, which generally favors the unitary, or B-phase-like, pairing symmetry. Upon further increasing doping, the non-unitary A-phase could be realized. In two dimensions, the unitary B state can be characterized as a state where the up (down) spin electrons are paired in the $p_x + ip_y$ ($p_x - ip_y$) state, so that the time-reversal symmetry is preserved. This state is similar to the topologically non-trivial state, characterized by the Z_2 invariant [19], found in quantized spin-Hall insulator [20]. In contrast, the time-reversal symmetry breaking A-phase could be realized in Sr_2RuO_4 partly because the carriers' density is high.

The topological nature of the proposed pairing state for LaOFeAs implies the existence of counter-propagating edge states which can be tested experimentally. In the bulk, the pairing state is fully gapped, and the STM experiment will show a full gap in the I-V characteristics. However, moving to the edge, the STM experiment will show a gapless spectrum, revealing the gapless edge states protected by the time-reversal symmetry. Most strikingly, in the presence of a magnetic impurity near the edge, the local density of states would show a gap again, due to the breaking of the time-reversal symmetry.

* * *

We acknowledge the valuable discussions with Y. P. Wang, N. L. Wang, J. L. Luo, H. H. Wen, T. Hughes, X. L. Qi, S. Raghu and D. Scalapino, and the supports from NSF of China and that from the 973 program of China (Nos. 2007CB925000 and 2006CB921300). SCZ acknowledges support by the NSF under grant No. DMR-0342832 and the US DOE, Office of Basic Energy Sciences under contract DE-AC03-76SF00515.

REFERENCES

[1] Nagamatsu J., Nakagawa N., Muranaka T., Zenitani Y. and Akimitsu J., *Nature (London)*, **410** (2001) 63.

[2] Rice T. M. and Sigrist M., *J. Phys.: Condens. Matter*, **7** (1995) L643; Luke G. M. *et al.*, *Nature*, **394** (1998) 558; Riseman T. M. *et al.*, *Nature*, **396** (1998) 242; Ishida K. *et al.*, *Nature*, **396** (1998) 658.

[3] Maeno Y. *et al.*, *Nature*, **372** (1994) 532.
[4] Takada K., Sakurai H., Muromachi E. T., Izumi F., Dilanian R. A. and Sasaki T., *Nature*, **422** (2003) 53; Schaak R. E., Klimczuk T., Foo M. L. and Cava R. J., *Nature*, **424** (2003) 527.
[5] Wang Y., Rogado N. S., Cava R. J. and Ong N. P., *Nature*, **423** (2003) 425.
[6] Kamihara Y. *et al.*, *J. Am. Chem. Soc.*, **128** (2006) 10012.
[7] Watanabe T. *et al.*, *Inorg. Chem.*, **46** (2007) 7719.
[8] Kamihara Y. *et al.*, *J. Am. Chem. Soc.*, **130** (2008) 3296.
[9] Zimmer B. I., Jeitschko W., Albering J. H., Glaum R. and Reehuis M., *J. Alloys Compd.*, **229** (1995) 238.
[10] Perdew J. P., Burke K. and Ernzerhof M., *Phys. Rev. Lett.*, **77** (1996) 3865.
[11] Vanderbilt D., *Phys. Rev. B*, **41** (1990) 7892.
[12] Blaha P. *et al.*, *An Augmented Plane Wave + Local Orbitals Program for Calculating Crystal Properties*, edited by Schwarz K. (TU Wien, Wien, Austria) 2001.
[13] Dong J. *et al.*, cond-mat/0803.3426 (2008).
[14] Oguchi T., *Phys. Rev. B*, **51** (1995) 1385; Singh D. J., *Phys. Rev. B*, **52** (1995) 1358.
[15] Fang Z., Solovyev I. V., Sawada H. and Terakura K., *Phys. Rev. B*, **59** (1999) 762.
[16] Lebégue S., *Phys. Rev. B*, **75** (2007) 035110.
[17] Yang H. *et al.*, cond-mat/0803.0623; Chen G. F. *et al.*, cond-mat/0803.0128 (2008).
[18] Anthony J. Leggett, *Rev. Mod. Phys.*, **47** (1975) 331.
[19] Kane C. L. and Mele E. J., *Phys. Rev. Lett.*, **95** (2005) 146802; 226801.
[20] Bernevig B. A., Hughes T. L. and Zhang S. C., *Science*, **314** (2006) 1757.